Intermetallics 23 (2012) 39–48

Contents lists available at SciVerse ScienceDirect

Intermetallics

journal homepage: www.elsevier.com/locate/intermet

# Electronic structure and mechanical properties of $Sc_3AC$ (A = Al, Ga, In, Tl) and $Sc_3BN$(B = Al, In): Ab-initio study

V. Kanchana*, Swetarekha Ram

*Department of Physics, Indian Institute of Technology Hyderabad, Ordnance Factory Campus, Yeddumailaram-502205, Andhra Pradesh, India*

ARTICLE INFO

*Article history:*
Received 18 July 2011
Received in revised form
18 November 2011
Accepted 21 December 2011
Available online 11 January 2012

*Keywords:*
A. Intermetallics
B. Elastic properties
E. Ab-initio calculations
E. Electronic structure
E. Mechanical properties

ABSTRACT

Systematic first principles calculations have been carried out to study the electronic structure and elastic properties of ternary scandium based antiperovskite carbides and nitrides. The calculated ground state properties agree well with the experimental and other theoretical results. The elastic constants are predicted from which all the related mechanical properties are calculated. From the analysis of the ratio of bulk modulus to shear modulus, we conclude that the above mentioned antiperovskites are brittle in nature with a considerable elastic anisotropy. The band structure shows a pronounced hybridization of Sc-*d* states with the *p* states of C or N at the Fermi level. It is observed that the changes brought about in the mechanical properties of Sc-based cubic inverse perovskites when replacing C by N are less pronounced than that for the Ti based antiperovskite carbides and nitrides, where it is quite noticeable. A possible reason for the change in behavior is also analyzed.



## 1. Introduction

Perovskite compounds comprise a large family of ternary phases, where a face-centered non-metallic atom is added to a metallic body centered cubic unit cell [1]. One of the most stable crystal structure for ternary and multinary compounds is the cubic perovskite structure. Among them, there exist a special type of perovskite having a metallic face-centered cubic structure with C or N atoms in body centered positions known as cubic anti or inverse perovskites [2]. Depending on their chemical composition, these ternary carbides or nitrides with an antiperovskite structure possess a wide range of interesting physical properties [3–7]. The cubic inverse perovskite nitrides comprise a relatively un-explored branch of the perovskite family, with captivating electronic properties that can be tuned to give rise to either a conducting, insulating or semiconducting behavior [8,9]. For example $AsNSr_3$, $SbNSr_3$ and $BiNSr_3$ are semiconductors with band gaps of 0.49, 0.31 and 0.26 eV respectively [10] and $XNCa_3$ (X = Ge, Sn, and Pb) are electrical conductors [11]. Apart from this, some of these antiperovskites such as $MgCNi_3$, $CdCNi_3$ compounds are found to be superconductors [6,12–14], which has been studied earlier, but the theoretical investigation on $AlCNi_3$ reveal that the compound is not a superconductor [15]. These available reports clearly indicate a wide range of properties existing among this class of compounds, which further emphasize the need to explore them. Nonetheless, there also exist several compounds with this antiperovskite structure possessing good mechanical properties, such as $Ti_3AlN$ [16], $Ti_3AlC$ [17], $Sc_3AlC$ [18], $Sc_3AlN$ [19], $Sc_3InN$ [20]. Though they are few in number, they attract the attention of experimentalists and theoreticians as it is well known that one can try to tune the electronic properties of nitrides by varying the electron concentration within the same crystal structure. By this, it is possible to achieve a situation with excess electrons or electron deficient systems such as $Ca_3AuN$ or $Ca_3TlN$ respectively, which will eventually be reflected in the physical behavior of the compounds. It is interesting to explore the above mentioned Ti and Sc based antiperovskite carbides and nitrides from different perspectives. As far as the Ti based systems are concerned, there is a recent ab-initio study available explaining the mechanical properties of $Ti_3AlY$ (Y = C, N) and predicting $Ti_3AlN$ to be ductile in contrast to $Ti_3AlC$ which is brittle [21]. Recently mechanical and thermodynamic stability of the isoelectronic ternary inverse perovskite $Sc_3EN$ (E = B, Al, Ga, In) has been studied [22]. Among these various Sc-based inverse perovskites, $Sc_3AlN$, $Sc_3GaN$ and $Sc_3InN$ phases were theoretically predicted to be dynamically stable through phonon spectra investigations, whereas $Sc_3BN$ was computed to have imaginary vibrational frequencies. Though some literatures are already available for Sc based nitrides and few carbides, we do not have a comparative study between them. In addition, it would

* Corresponding author. Tel.: +91 40 23016019; fax: +91 40 23016032.
*E-mail address:* kanchana@iith.ac.in (V. Kanchana).

0966-9795/$ – see front matter © 2011 Elsevier Ltd. All rights reserved.
doi:10.1016/j.intermet.2011.12.014

be interesting to investigate the role of C and N in $Sc_3XY$, where X = Al, Ga, In, Tl and Y = C and N. Here in the present work, we report a complete study of the above mentioned compounds except $Sc_3GaN$ and $Sc_3TlN$ due to lack of experimental data and try to compare it with $Ti_3AlC$ and $Ti_3AlN$. The main emphasis is to find the role of nitrogen in the Sc based antiperovskite nitrides and we clearly show that the effect of replacing C by N is negligible in Sc based compounds in contrast to Ti based compounds, where the compound changes the nature from brittle to ductile when replacing C by N. A possible reason for this is speculated using the band structure, density of states and difference valance electron-density plots. The rest of this paper is organized in the following manner. The second section describes the computational and structural details. Results about elastic, electronic properties and Fermi surface studies are elaborated in the third section and finally the last section concludes the paper.

## 2. Computational details

In this work, the all-electron full-potential linear augmented plane wave plus local orbital method as implemented in WIEN2k [23,24] has been used to calculate the total energies as well as the basic ground state properties. The exchange–correlation potential was calculated within the generalized gradient approximation (GGA) according to the Perdew-Burke-Ernzerhof parametrization [25]. In all the calculations, we used a muffin-tin radius of 2.00 a.u for Sc, 2.3 a.u for X (Al, Ga, In, Tl) and 1.8 a.u for Y (C, N). The maximum $l$ value used in the expansion of the crystal potential and electron-density within muffin-tin sphere was $l = 10$. In the interstitial region, a plane wave expansion with $R_{MT}K_{max} = 8$ was used for all the investigated systems. The potential and the charge density were Fourier expanded up to $G_{max} = 8$. We carried out convergence tests for the higher $G_{max}$ values and found no significant changes in the calculated properties. A modified tetrahedron method [26] was applied to integrate inside the Brillouin zone (BZ) and for $k$ -space integration, a $(26 \times 26 \times 26)$ mesh was used resulting in 560 $k$ -points in the irreducible part of the BZ according to the Monkhorst–Pack scheme [27]. Birch–Murnaghan equation of states (EOS) [28] was used to fit the total energies as a function of primitive unit cell volume to obtain the bulk modulus and the equilibrium lattice parameter for the investigated systems.

In addition, the Fermi surfaces of $Sc_3XY$ (X = Al, Ga, In, Tl; Y = C, N) were also plotted. The calculations for generating the Fermi surface were carried out by using a plane wave pseudopotential method [29,30] as implemented in the QUANTUM-ESPRESSO simulation package (PWSCF) [31]. The generalized gradient approximation (GGA) to the exchange–correlation functional is employed using an ultrasoft pseudopotential. In order to deal with the possible convergence problem for metals, a smearing technique was employed using the Methfessel–Paxton (MP) scheme, with the smearing parameter set to 0.04 Ry and the convergence tests give a kinetic energy cutoff $E_{cutoff}$ as 40 Ry. The $(16 \times 16 \times 16)$ mesh was used to obtain the smooth Fermi surface for the bands which cross the Fermi level. The smooth three dimensional (3D) Fermi surface plots were generated with the help of the Xcrysden molecular structure visualization program [32].

All the $Sc_3XY$ compounds under study crystallize in the inverse perovskite structure. The inverse perovskite is a cubic crystal structure with light metal atoms X (Al, Ga, In, Tl) at the cube corner site, heavy metal atoms (Sc) at face-centered position and the nonmetal atoms (C, N ) in the body centered position. The atomic arrangement of such a cubic structure is basically similar to that of a common perovskite, where the heavy metal atom (Sc) has exchanged positions with nonmetal atoms (C, N). The crystal structure of $Sc_3XY$ corresponds to the filled-up $Cu_3Au$ type [18] of space group pm-3m (221). The Wyckoff positions of the Sc atom is (1/2, 1/2, 0); X = (0, 0, 0) and Y = (1/2, 1/2, 1/2).

## 3. Results and discussion

To obtain the basic ground state properties, we calculated the total energies as a function of lattice parameter for all these compounds $Sc_3XY$ and fitted to the Birch–Murnaghan equation of state [28]. The calculated structural parameters along with the experimental and other theoretical values of all the $Sc_3XY$ compounds are reported in Table 1. Our calculated lattice parameter is in good agreement with the experimental and other theoretical values. Our theoretical lattice parameters are slightly larger than the experimental values with the maximum error of 1.1% for $Sc_3TlC$ and minimum of 0.22% for $Sc_3GaC$. It is well known that GGA overestimates the equilibrium lattice constant by 1–2%. We can also observe that substitution of C by N reduce the equilibrium volume by about 6.1% for Al containing compounds and 5.8% for In containing compounds. The same reduction in volume is also observed in our earlier study for $Ti_3AlY$ (Y = C,N) [21].

### 3.1. Elastic constants, and mechanical properties

The calculated bulk moduli and the elastic constants of the investigated system are reported in Table 1. Our calculated bulk moduli agree quite well with other available theoretical values. We observed that the values of bulk moduli increases when replacing C by N and decreases from Al → Ga → In → Tl, in both carbide and nitride series in our calculation. To study the structural stability of the investigated systems, we calculated the formation energy $\Delta H_f$. At zero temperature, there is no entropy contribution to the free energy; therefore, the heat of formation can be obtained from the following relation,

$$\Delta H_f^{X_3YZ} = \left[H_{Total}^{X_3YZ} - \left(3H_{solid}^{X} + H_{solid}^{Y} + H_{solid}^{Z}\right)\right] \quad (1)$$

and are reported in Table 1. The formation energy is found to be negative for the above mentioned compounds, indicating that their formation is exothermic and the compounds are structurally stable as evident from our calculated values of $\Delta H_f$. Further, we find $\Delta H_f$ to decrease by replacing C with N as well as by replacing Al by Ga, In and Tl. Though we find $\Delta H_f$ to reduce from Al → Ga → In, the corresponding value of $Sc_3TlC$ is found to be little higher than In, which is similar to the trend observed in the case of $Ti_2MC$(M = Al, Ga, In, Tl) [33].

As a next step, we look at the mechanical stability of the system and the elastic constants are fundamental parameters for describing the mechanical properties of materials. Cubic lattices have three independent elastic constants [34–36] namely $C_{11}$, $C_{12}$ and $C_{44}$. The criteria for mechanical stability of any compound is that the strain energy should be positive, which imposes further restriction on the values of the elastic constants [37,38] such as

$$C_{11} > C_{12}, C_{44} > 0, C_{11} + 2C_{12} > 0.$$

The above mentioned criteria for mechanical stability are satisfied by the calculated elastic constants of all the compounds under study and are reported in Table 1.

Once the single crystal elastic constants are computed, the related poly-crystalline properties such as Young's modulus ($E$), Shear modulus ($G_H$), Anisotropy factor (A) were derived using the standard relations,

**Table 1**
Calculated ground state, and elastic properties of $Sc_3XY$ at the theoretical equilibrium volume (lattice parameter ($a$), Volume ($V$), density ($\rho$), Bulk modulus ($B$), DOS ($N(E_F)$) in (states/eV), Formation energy ($\Delta H_f$) in eV/atom, Young's modulus ($E$), Poisson's ratio ($\sigma$), Anisotropy factor (A), Cauchy's pressure (CP)).

| Properties | | $Sc_3AlC$ | $Sc_3GaC$ | $Sc_3InC$ | $Sc_3TlC$ | $Sc_3AlN$ | $Sc_3InN$ |
|---|---|---|---|---|---|---|---|
| $a$ (Å) | calc. | 4.51 | 4.48 | 4.56 | 4.56 | 4.42 | 4.47 |
| | expt. | 4.48[a] | 4.47[b] | 4.54[b] | 4.51[b] | 4.40[c] | 4.45[d] |
| | others | 4.48[e] | – | – | – | 4.39[e],4.37[f] | 4.41[f] |
| | | | | | | 4.42[g] | |
| $V$ (Å$^3$) | | 91.93 | 89.92 | 94.82 | 94.82 | 86.35 | 89.31 |
| $\rho$ (g/cm$^3$) | | 3.15 | 4.00 | 4.58 | 6.15 | 3.38 | 4.90 |
| $B$ (GPa) | | 99.91 | 99.07 | 96.06 | 94.41 | 114.76 | 106.11 |
| | | 101.6[e] | – | – | – | 114.25[f],106.6[g] | 115.21[f] |
| | | – | – | – | – | 111.4[e] | |
| $N(E_F)$ | | 0.553 | 0.426 | 0.427 | 0.311 | 2.476 | 2.470 |
| $\Delta H_f$ | | −3.1 | −3.56 | −3.64 | −3.46 | −5.5 | −5.82 |
| $C_{11}$ (GPa) | | 220 | 227 | 213 | 212 | 241 | 210 |
| | | | – | – | – | 234[f] | 239[f] |
| | | 225[e] | – | – | – | 230[e] | |
| | | | – | – | – | 223[g] | |
| $C_{12}$ (GPa) | | 40 | 35 | 38 | 36 | 52 | 54 |
| | | 40[e] | – | – | – | 50[e], 54[f] | 54[f] |
| | | | – | – | – | 48[g] | – |
| $C_{44}$ (GPa) | | 79 | 76 | 81 | 80 | 76 | 80 |
| | | | – | – | – | 88[f] | 91[f] |
| | | 81[e] | – | – | – | 84[e] | |
| | | | – | – | – | 86[g] | – |
| E (GPa) | | 195 | 195 | 193 | 192 | 201 | 193 |
| | | 199.7[e] | – | – | – | 205.2[e] | |
| | | | – | – | – | 211.33[f] | 216.88[f] |
| $G_H$ (GPa) | | 83.26 | 83.44 | 82.69 | 82.74 | 83.02 | 80.39 |
| $G_H/B$ | | 0.83 | 0.84 | 0.86 | 0.88 | 0.72 | 0.76 |
| $\sigma$ | | 0.17 | 0.17 | 0.17 | 0.16 | 0.21 | 0.20 |
| A | | 0.87 | 0.79 | 0.91 | 0.90 | 0.81 | 1.06 |
| | | 0.88[e] | – | – | – | 0.94[e] | |
| CP | | −39.15 | −40.90 | −41.90 | −43.66 | −24.37 | −27.94 |

[a] Ref [18].
[b] Ref [48].
[c] Ref [36].
[d] Ref [20].
[e] Ref [46].
[f] Ref [45].
[g] Ref [49].

$$A_G = \frac{2C_{44}}{C_{11} - C_{44}} \tag{2}$$

$$E = \frac{3BG_H}{3BG_H + G_H} \tag{3}$$

$$G_H = \frac{G_R + G_V}{2} \tag{4}$$

$$G_V = \frac{3C_{44} + C_{11} - C12}{5} \tag{5}$$

$$G_R = \frac{5(C_{11} - C_{12})C_{44}}{4C_{44} + 3(C_{11} - C_{12})} \tag{6}$$

According to Hill [39], the arithmetic average of the Voigt ($G_V$) [40] and Reuss ($G_R$) [41] values can be used to estimate the average shear modulus which is represented as $G_H$. The derived quantities from the elastic constants are given in Table 1 and the related mechanical behavior of the materials under study is explained here. From our reported value in Table 1 we can see that, the Young's modulus of all the $Sc_3XY$ compounds are nearly the same. For a completely isotropic system, the anisotropy factor (A) takes the value of unity and any deviation from unity measures the degree of elastic anisotropy. So from the anisotropic factor (A) as reported in Table 1, all the compounds $Sc_3XY$ are elastically anisotropic. The negative (positive) value of Cauchy's pressure ($C_{12}$–$C_{44}$) determines the brittle (ductile) nature of the compounds. The Pugh's ratio ($G_H$/B) is yet another index for explaining the ductile and brittle nature of the compounds. The high (low) $G_H$/B ratio is associated with the brittle (ductile) nature of the materials [42]. The critical number that separates the ductile and brittle nature was found to be 0.57. According to above description, $Sc_3XY$ are brittle in nature, which is clearly seen from the Table 1. In addition, the extent of covalent character also has further impact on the brittle nature of the compounds. From our calculated values of the Cauchy's pressure we can see that the covalency slightly increases as we go from

**Table 2**
Calculated sound velocity ($v_t$, $v_l$, $v_m$ are transverse, longitudinal and mean sound velocities respectively) and Debye temperature $\Theta_D$ of $Sc_3XY$ at the theoretical equilibrium volume.

| properties | $Sc_3AlC$ | $Sc_3GaC$ | $Sc_3InC$ | $Sc_3TlC$ | $Sc_3AlN$ | $Sc_3InN$ |
|---|---|---|---|---|---|---|
| $v_t$ (km/s) | 5.14 | 4.57 | 4.25 | 3.67 | 4.96 | 4.05 |
| | – | – | – | – | 5.04[a] | 4.23[a] |
| $v_l$ (km/s) | 8.19 | 7.25 | 6.71 | 5.77 | 8.17 | 6.60 |
| | – | – | – | | 8.16[a] | 6.82[a] |
| $v_m$ (km/s) | 5.66 | 5.03 | 4.67 | 4.03 | 5.48 | 4.47 |
| $\Theta_D$ (K) | 639 | 571 | 522 | 450 | 631 | 509 |
| | – | – | – | – | 647.15[a] | 538.33[a] |

[a] Ref [45].

Al → Ga → In → Tl, which eventually increases the brittleness of the compounds. This is further evident from the difference valence electron-density plots as shown in Fig. 3. But when we replace C with N there is a very slight decrease in the covalency of Sc-based nitrides in contrary to $Ti_3AlC$ and $Ti_3AlN$, where $Ti_3AlC$ is more covalent and $Ti_3AlN$ is more ionic [21] leading to a ductile behavior in the latter. The stability of the crystal against shear generally depends on Poisson's ratio ($\sigma$) which takes the value −1 as lower bound and 0.5 as upper bound. The lower bound indicates where the material does not change its shape and the upper bound indicates when the volume remains unchanged. The Poisson's ratio ($\sigma$) is defined by using Hill's limit [39] with the following equation.

$$\sigma = \frac{3B - 2G_H}{2(3B + G_H)} \tag{7}$$

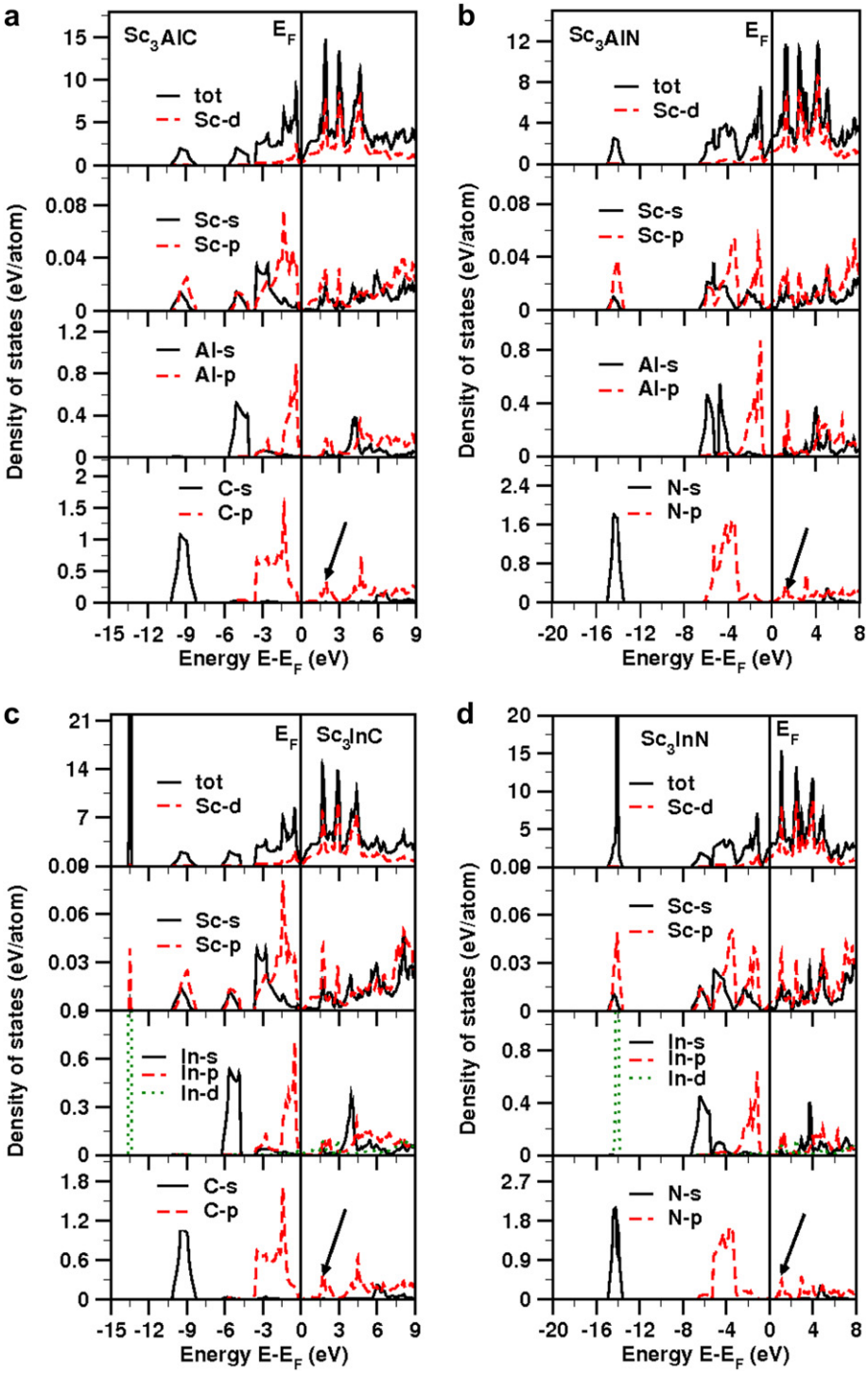


**Fig. 1.** Partial Density of States of $Sc_3XY$ and $Ti_3AlY$ (Arrow mark represent the position of hybridized Sc(Ti)-d and C(N)-p states in conduction band). (For interpretation of the references to color in this figure legend, the reader is referred to the web version of this article.)

So the stability of these compounds is further confirmed from the value of $\sigma$ as reported in Table 1. Debye temperature ($\Theta_D$) is one of the most important parameter and it determines the thermal characteristics of materials. The Debye temperature can be defined in terms of the mean sound velocity and gives explicit information about lattice vibration [43,44] and can be computed directly from the given relation.

$$\Theta_D = \frac{h}{k}\left[\frac{3n}{4\pi}\left(\frac{N_A\rho}{M}\right)\right]^{1/3} v_m \tag{8}$$

Where 'h' is the Planck's constant, 'k' is the Boltzmann's constant, '$N_A$' is the Avogadro's number, '$\rho$' is the density, '$M$' is the molecular weight, 'n' is the number of atoms in the unit cell, and '$v_m$' is the mean sound velocity, which can be calculated by using the following relation.

$$v_m = \left[\frac{1}{3}\left(\frac{2}{v_t^3}+\frac{1}{v_l^3}\right)\right]^{-1/3} \tag{9}$$

where '$v_l$ ' and '$v_t$ ' are the longitudinal and transverse sound velocities obtained using the shear modulus $G_H$ and the bulk modulus B.

$$v_l = \sqrt{\frac{\left(B+\frac{4}{3}G_H\right)}{\rho}} \tag{10}$$

$$v_t = \sqrt{\frac{G_H}{\rho}} \tag{11}$$

From the value of $\Theta_D$ as reported in Table 2, we can see that, there is a negligible difference between the Sc based cubic inverse perovskite carbides and nitrides. But we could find a progressive decrease in the mean sound velocity ($v_m$) and $\Theta_D$ values in replacing X by Al → Ga → In → Tl in $Sc_3XC$. A similar trend is also seen among the $Sc_3XN$ by Mattesini [45]. No appreciable change is observed in replacing C by N for a particular X in Sc based compounds. This is quite contrary to Ti based compounds and a possible reason is speculated in the next section from the electronic band structure and density of states.

### 3.2. Electronic properties

The overall electronic structure of all the compounds remains the same with slight changes which are discussed below. To capture and discuss the slight changes brought about by varying Al → Ga → In → Tl and by replacing C with N, we present the Density of States (DOS), band structure and valence electron-density plots of $Sc_3AlC(N)$ and $Sc_3InC(N)$ along with the $Ti_3AlC(N)$ in Fig. 1, Fig. 2 and Fig. 3 respectively. The higher lying electronic states which extend from −10 eV to 0 eV for $Sc_3XC$ and from −15 eV to 0 eV for $Sc_3XN$ as shown in Fig. 1, relate both the weak metal–metal (Sc–X) and strong metal–nonmetal (Sc–Y) interactions. The overall electronic structure of the remaining carbides and nitrides under study also remains the same. In all $Sc_3XY$ compounds, the states lying just below the Fermi level are mainly due to the hybridization of Sc-s, p, d, X-p, d and Y-p states. But the states lying on the Fermi level are mainly due to the Sc-d and a small contribution from C-p (or N-p) like states in $Sc_3AlC$ and $Sc_3AlN$ and in rest of the compounds there is also a small contribution due to X-d states. Again in all cubic inverse perovskite carbides the C-p states lie just below the $E_F$ and there is a 5 eV energy gap in between C-s and C-p states, while the N-p states are still 2 eV deeper in energy and there is 7 eV energy gap in between N-s and p states. As a result, from the DOS one could see that the extent of hybridization of Sc-d and N-p is weaker than

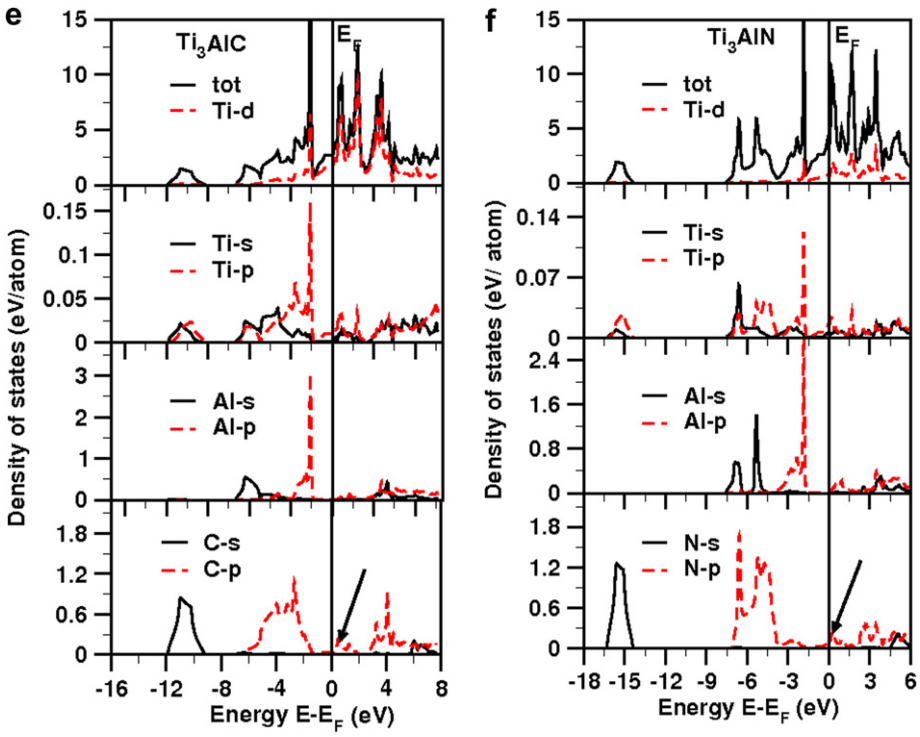


**Fig. 1.** (*continued*).

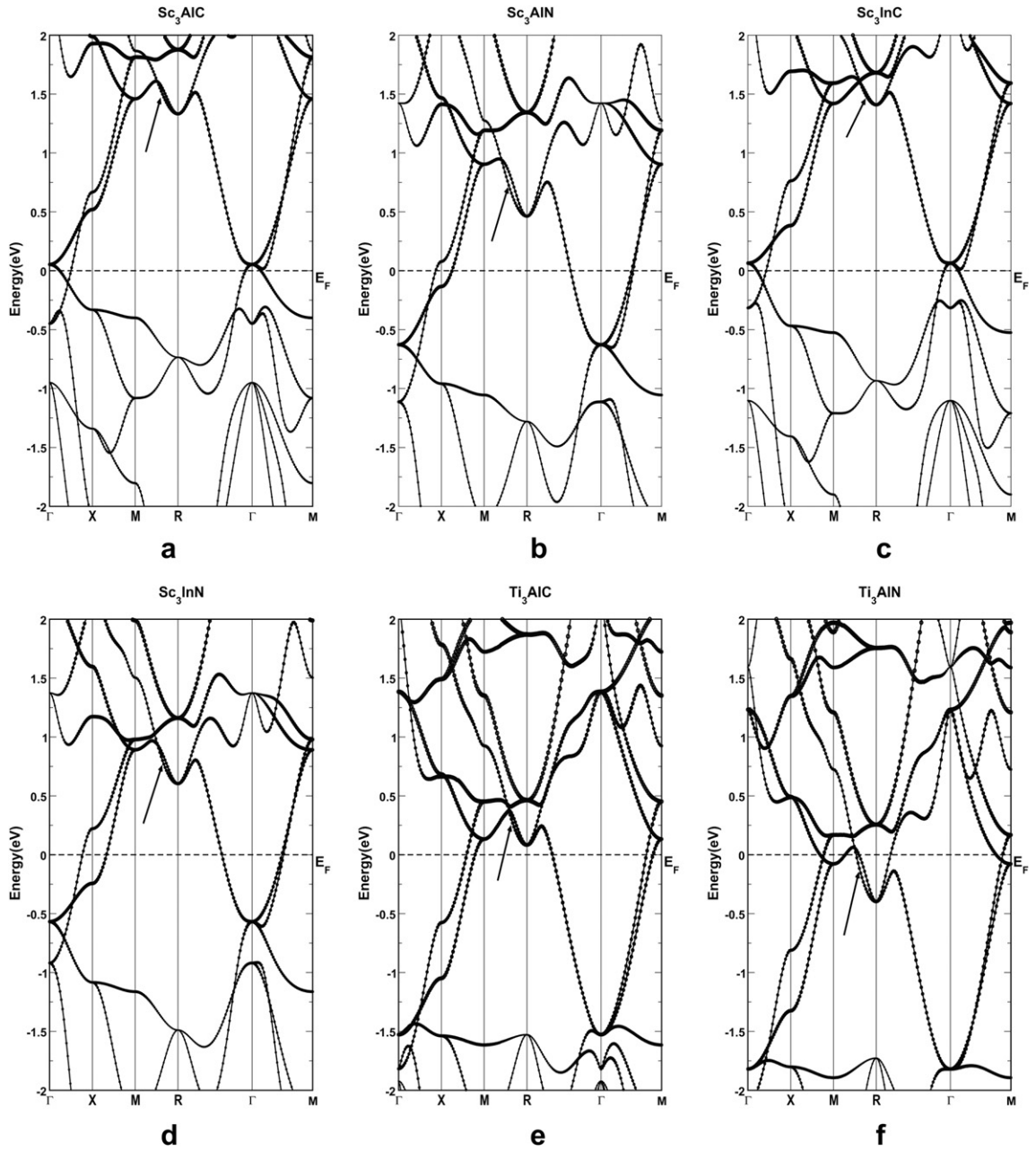


**Fig. 2.** Band structure of $Sc_3XY$ and $Ti_3AlY$ (Arrow mark represent the position of hybridized Sc(Ti)-d and C(N)-p states in conduction band).

the Sc-d and C-p states leading to an increased covalent character in the bonding between Sc and C atoms, which is more evident from the difference valence electron-density plots as shown in Fig. 3. In addition, from the DOS one could see the existence of pseudo gap in all the Sc-based carbides under study. More interestingly, we could see that the band present close to the Fermi level, is a rigid band (shown as arrow mark in Fig. 2) and replacing C by N, results in the shifting of the Fermi level, eventually leading to band filling and the pseudo gap disappears in the case of nitrides which can also be seen from the Fermi surface plots of Sc based carbides and nitrides. The main point which we would like to address here is the possible reason for the behavior change in $Ti_3AlN$, which is quite different from $Ti_3AlC$ and other Sc based compounds under study. In $Sc_3XY$ and in $Ti_3AlC$, the contribution from hybridized Sc or Ti-d and C or N-p states (shown as arrow mark in Fig. 1) at Fermi level is less as they are present much higher in the conduction band when compared with $Ti_3AlN$, where these hybridized states shift down and lie well inside the valence band which eventually leads to the change in the observed physical properties. This observed change is mainly due to the presence of an extra electron in N leading band filling and is further evident and clear from the band structure of the compounds as shown in Fig. 2. But when we try to analyze the same effect in Sc based compounds, we could see that these states (hybridized Sc-d and C(N)-p) lie well above the Fermi level and replacement of C by N does not produce any significant change in physical properties. Fermi surface plots are also further strengthens this point clearly showing the formation of the additional electron pocket at the R point in the Brillouin zone for $Ti_3AlN$, which will be discussed elaborately in the succeeding section.

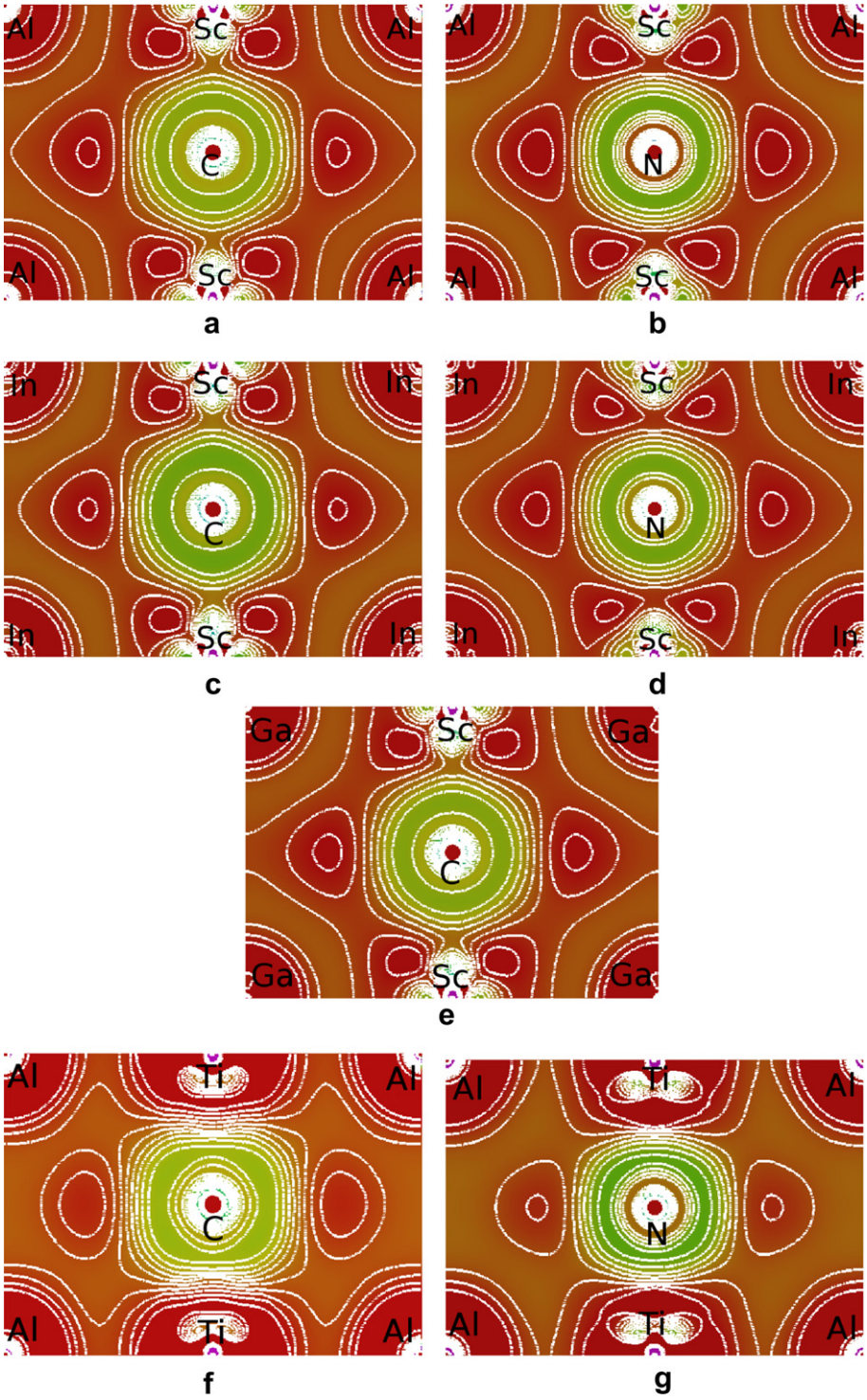


**Fig. 3.** Difference valence electron-density plot of $Sc_3AlY$ [a,b], $Sc_3InY$ [c,d], $Sc_3GaC$ [e] and $Ti_3AlY$ [f,g] in [110] plane. (For interpretation of the references to color in this figure legend, the reader is referred to the web version of this article.)

Since for free electrons, the electrical conductivity is directly proportional to the density of states ($N(E_F)$) at Fermi level, we calculated the total $N(E_F)$ of the investigated systems and are reported in Table 1. Based on the above description and from the value of total $N(E_F)$, the conductivity decreases from Al → In → Tl in carbides series. But our calculated value of $N(E_F)$ indicates $Sc_3GaC$ to have slightly lower conductivity than $Sc_3AlC$ and $Sc_3InC$. Similarly the electrical conductivity may decrease from the Al to In for Sc-based nitrides. The trend in conductivity of Sc-based carbides and nitrides as observed here is well comparable with Sc-based nitrides observed by Mattesini et al. [45]. We also observed an increase in $N(E_F)$ by replacing C with N for the investigated systems, which again indicates the increase in electrical conductivity for Sc-based nitrides compared to Sc-based

carbides. Fig. 3 shows the difference valence electron-density plots in [110] plane for $Sc_3XY$ which is nothing but crystalline minus superposed atomic densities. A proper understanding of the electronic structure particularly the bonding nature of the systems studied is obtained using the charge density plots. From the Fig. 3, we could observe the presence of covalent bonding between Sc–C(N) in $Sc_3XY$. When we replace C with N, the extent of covalency is reduced in nitrides as compared to carbides, which can be evident from the nearly spherical charge distribution seen around the N atom. But if we tend to analyze the bonding prevailing between the Sc and X (Al, Ga, In, Tl), we observe mixed ionic-covalent character present between the comprising elements. By replacing Al with Ga, In and Tl among the Sc-based carbides we observe the ionic character present between Sc–Ga to decrease as compared with other carbides as shown in Fig. 3. This is mainly due to higher electronegativity of Ga and the smaller ionic radius of Ga among the X atoms resulting in the shortest bond length of Sc–Ga. The same trend is also observed for Sc-based nitrides by Mattesini et al. [45]. From the above discussion we conclude that the bonding nature of the investigated system is of mixed covalent-ionic type and our results are also in good agreement with other related compounds [11,47]. Altogether, we could observe that by increasing atomic number (Z) and by replacing X down the column in the periodic table, the covalent character increases and across the period by replacing Y, the covalent character of Sc-based cubic inverse perovskites decreases. But the replacement of Y (C with N) in $Ti_3AlC$ completely changes the bonding nature to be less covalent in the case of $Ti_3AlN$, making the compound ductile in contrast to $Ti_3AlC$, which is brittle in nature, as seen in the valence electron-density plots in Fig. 3 and also explained earlier [21].

### 3.3. Fermi surface study

The Fermi surface (FS) of $Sc_3XY$ and $Ti_3AlY$ were plotted for the bands which cross the Fermi level, and this is mainly due to Sc-d, X-d (X = Ga, In, Tl) and C-p or N-p states for $Sc_3XY$ and Ti-d and C-p or N-p states for $Ti_3AlY$, the corresponding Fermi surfaces are shown in Fig. 4. From the Fermi surface plots one can see that, the Fermi surface topology changes by replacing C with N and also for replacing Sc by Ti. But Fermi surface topology remains almost unaltered for X varying from Al to In in Sc based carbides and nitrides, which indicates that the major contribution arises from Sc-d or Ti-d states and C(N)-p states on the Fermi level which is also evident from DOS in Fig. 1.

As discussed earlier, the main interest of the present work lies in highlighting the effect of varying X and Y in the Sc based compounds under study. It is clearly seen from Fig. 4, that the Fermi surface topology remains unchanged on the whole except varying in size, when we replace X from Al to Tl. In accordance to the fact that the X-d character increases as we replace Al by Ga, In, Tl, we could see that reflecting in the Fermi surface as $Sc_3InC$ has a larger hole packet at Γ and a smaller electron packet along Γ → X direction, when compared to $Sc_3AlC$. From the Fermi surface, it is clear that all the Sc-based carbides presented here are pseudo gap materials.

Next, when looking at replacing C by N, we could see that bands crossing the Fermi level at Γ and along Γ → X direction shifts down, which eventually leads to an electron pocket at the Γ point in the $Sc_3AlN$, in contrary to a hole pocket in $Sc_3AlC$. Likewise, we could also find a shift of bands along Γ → X direction leading to an interconnected tubular like electron sheet in the case of $Sc_3XN$, which was not that pronounced in the case of $Sc_3XC$. Among the Sc based nitrides, replacing X from Al to Tl results in wider tubular sheets and a more spherical electron pocket as evident in $Sc_3InN$.

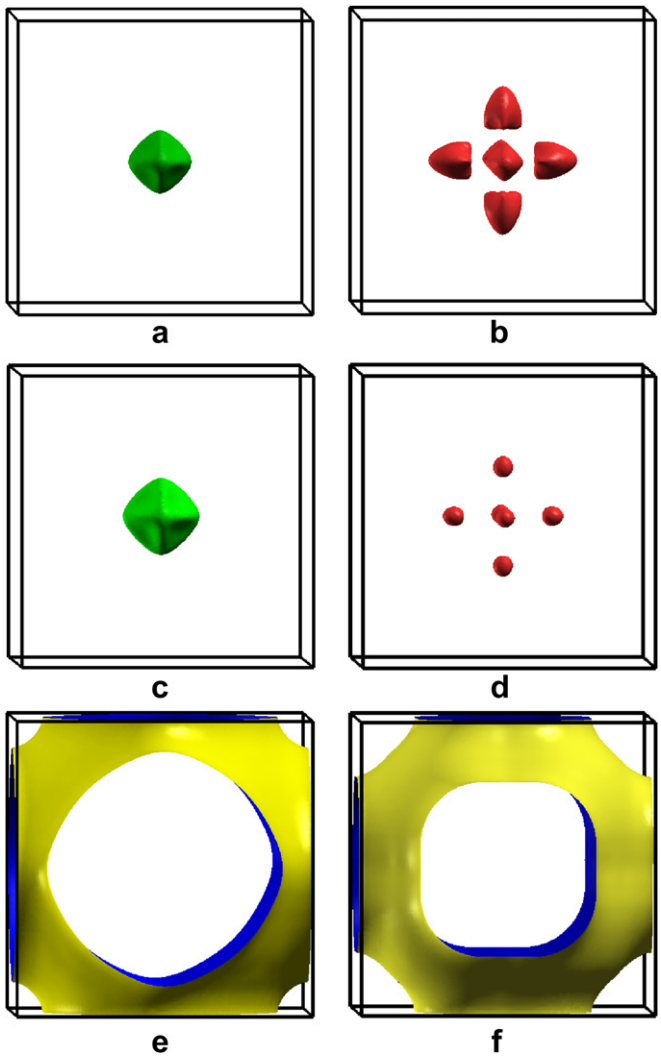


**Fig. 4.** Fermi surface of $Sc_3AlC$ [a,b], $Sc_3InC$ [c,d], $Ti_3AlC$ [e,f], $Sc_3AlN$ [g,h], $Sc_3InN$ [i,j], $Ti_3AlN$ [k,l,m], Here the center of the cube (Brillouin zone) represents the 'Γ' point, middle of the edge is 'M' point, corner of the cube is 'R' point and the center of face is 'X' point. (For interpretation of the references to color in this figure legend, the reader is referred to the web version of this article.)

The main focus is to account for the different behavior observed in $Ti_3AlY$, which can also be visualized from the Fermi surface plots. This can be done by comparing the Fermi surface plots of $Sc_3XY$ with $Ti_3AlC$ and $Ti_3AlN$. From Fig. 2, it is clear that the hybridized Sc(Ti)-d and C(N)-p bands along M to R high symmetry point, shown by an arrow in the figure, plays a vital role in differentiating $Ti_3AlN$ from $Ti_3AlC$ and other Sc based carbides and nitrides. As discussed earlier, this is a rigid band, and on replacing C by N, this band is occupied due to band filling, which eventually leads to an additional electron pocket at the R point, representing the third Fermi surface in $Ti_3AlN$, which is absent in all the other compounds, in addition to other two bands which crosses the Fermi level as shown in Fig. 4(m). This results in additional electrons available for conduction leading to the change in the physical properties observed in $Ti_3AlN$. As this hybridized state lie well above the Fermi level in all the other Sc based compounds, replacing C by N does not play a significant role in improving the

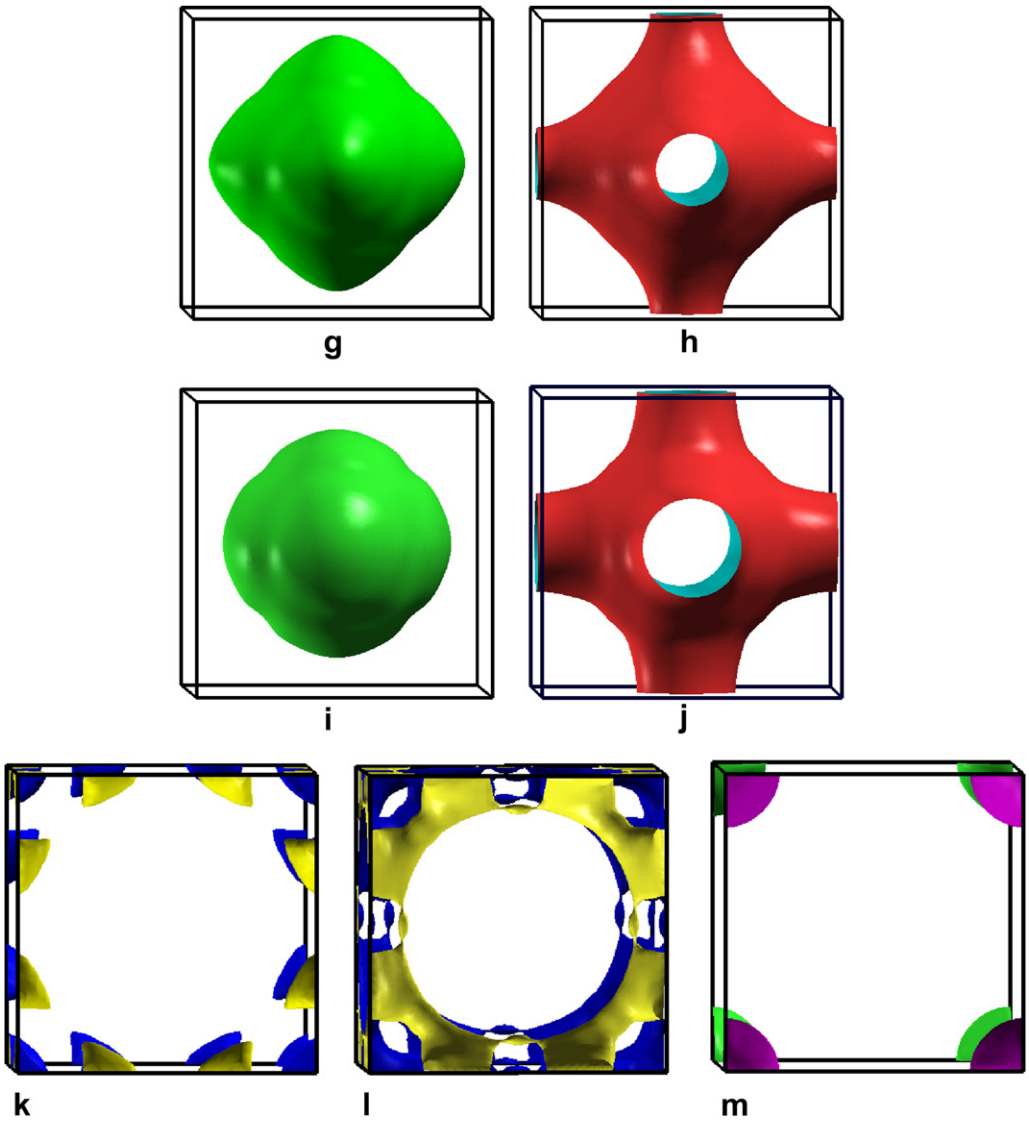


**Fig. 4.** (*continued*).

mechanical properties of these compounds and, which is also evident from the calculated elastic properties as reported in Table 1 and discussed earlier.

## 4. Conclusion

An ab-initio study of cubic inverse perovskites were carried out using the all-electron full-potential linear augmented plane wave plus local orbital method within the generalized gradient approximation. We have studied the structural, electronic, elastic, mechanical properties of Sc based carbides and nitrides. Our calculated ground state properties agree well with the experimental and other theoretical values. Our calculations show that replacing C by N changes the Fermi surface topology but structural, elastic and mechanical properties remain unchanged in our investigated compounds $Sc_3XY$ which is completely different from $Ti_3AlY$ (Y = C, N), where the mechanical behavior changes from ductile to brittle in replacing N by C. The possible reason for this change in behavior is analyzed from different perspectives. The high $G_H/B$ ratio shows that these materials are brittle in nature. The stability of the $Sc_3XY$ compounds was confirmed from the Poisson's ratio value. The sound velocity and Debye temperature were also calculated for the Sc-based cubic inverse perovskites under study. From the above study, we conclude that $Ti_3AlN$ is the only compound which is ductile and the possible reason is also reported.

## References

[1] Rose G. Ann Phys Chem 1839;48:551–72.
[2] Jäger J, Stahl D, Schmidt PC, Kniep R. Angew Chem Int Ed Engl 1993;32:709–10.
[3] Ivanovskii AL. Russ Chem Rev 1996;65(6):461–78.
[4] Kim WS, Chi EO, Kim JC, Choi HS, Hur NH. Solid State Commun 2001;119:507.
[5] Chi EO, Kim WS, Hur NH, Jung D. Solid State Commun 2001;120:307.
[6] He T, Huang Q, Ramirez AP, Wang Y, Regan KA, Rogado N, et al. Nature 2001;411:54–6.
[7] Chi EO, Kim WS, Hur NH, Jung D. Solid State Commun 2002;121:309–12.
[8] Chern MY, Vennos DA, Disalvo FJ. J Solid State Chem 1992;96:415.
[9] Niewa R, Schnelle W, Wagner FR, Anorg Z. Allg Chem 2001;627:365.
[10] Haddadi K, Bouhemadou A, Louail L, Rahal F, Maabed S. Comput Mat Sci 2009;46:881–6.
[11] Haddadi K, Bouhemadou A, Louail L, Medkour Y. Solid State Commun 2009;149:619–24.
[12] Uehara M, Amano T, Takano S, Kori T, Yamazaki T, Kimishima Y. Physica C 2006;440:6.
[13] Uehara M, Yamazaki T, Kori T, Kashida T, Kimishima Y, Hase I. J Phys Soc Jpn 2007;76:034714.

[14] Vaitheeswaran G, Kanchana V, Svane A, Delin A. J Phys Condens Matter 2007; 19:326214.
[15] Okoye CMI. Solid State Commun 2005;136:605.
[16] Schuster JC, Bauer J. J Solid State Chem 1984;53:260.
[17] Tian WH, Nemoto M. Intermetallics 1999;7:1261.
[18] Nowotny H. Prog Solid State Chem 1970;2:27.
[19] Höglund C, Birch J, Beckers M, Alling B, Czigány ZS, Mücklich A, et al. Eur J Inorg Chem 2008;8:1193.
[20] Kirchner M, Schnelle W, Wagner FR, Niewa R. Solid State Sci 2003;5:1247.
[21] Kanchana V. Euro Phys Lett 2009;87:26006.
[22] Mikhaylushkin AS, Höglund C, Birch J, Czigany Zs, Hultman L, Simak SI, et al. Phys Rev B 2009;79:134107.
[23] Blaha P, Schwarz K, Sorantin PI, Tricky SB. Comput Phys Commun 1990;59:399.
[24] Blaha P, Schwarz K, Madsen GKH, Kvasnicka D, Luitz J. In: Schwarz K, editor. WIEN2K, an augmented plane wave plus local orbitals programe for calculating crystal properties. Austria: Techn. Universität wien; 2001.
[25] Perdew JP, Burke K, Ernzerhof M. Phys Rev Lett 1996;77:3865.
[26] Blöchl PE, Jepsen O, Andersen OK. Phys Rev B 1994;49:16223.
[27] Monkhorst HJ, Pack JD. Phys Rev B 1976;13:5188.
[28] Birch F. Phys Rev 1947;71:809.
[29] Hohenberg P, Kohn W. Phys Rev 1964;136:864.
[30] Kohn W, Sham LJ. Phys Rev 1965;140. A1133.
[31] Giannozzi P, Baroni S, Bonini N, Calandra M, Car R, Cavazzoni C, et al. J Phys Condens Matter 2009;21:395502.
[32] Kokalj A. Comput Mater Sci 2003;28:155.
[33] Hug G. Phys Rev B 2006;74:184113.
[34] Nye JF. Physical properties of crystal: their representation by tensors and matrices. Oxford: Oxford University Press; 1985.
[35] Mattesini M, Ahuja R, Johansson B. Phys Rev B 2003;68:184108.
[36] Mattesini M, Soler JM, Yndurain F. Phys Rev B 2006;73:094111.
[37] Eriksson O. Electronic structure calculation of phase stability: cohesive and elastic properties. Encyclopedia of Materials: Science and Technology. Amsterdam: Elsevier; 2003. p. 1–11.
[38] Wallace DC. Thermodynamics of crystals. New York: Wiley; 1972.
[39] Hill R. Proc Phys Soc London 1952;65:350.
[40] voigt W. Ann Phys (Leipzig) 1889;38:573.
[41] Reuss A, Angew Z. Math Phys 1929;9:49.
[42] Pugh SF. Philos Mag 1954;45:823.
[43] Ibrahim AM. Nucl Instrum Methods Phys Res B 1988;34:135.
[44] Anderson OL. J Phys Chem Solid 1963;24:909.
[45] Mattesini M, Magnuson M, Tasnádi F, Höglund C, Abrikosov IA, Hultman L. Phys Rev B 2009;79:125122.
[46] Medkour Y, Roumili A, Maouche D, Saoudi A. Solid State Comm 2009;149: 1840–2.
[47] Martin M, Mattesini M, Höglund C, Abrikosov Igor A, Birch Jens, Hultman Lars. Phys Rev B 2008;78:235102.
[48] Stadelmaier HH. Metallkde Z 1961;52:758.
[49] Baĝci S, Yalçin BG, Tütüncü HM, Srivastava GP. Phys Rev B 2010;81:054523.